methods

Kdo_2-Lipid A of *Escherichia coli*, a defined endotoxin that activates macrophages via TLR-4

Christian R. H. Raetz,* Teresa A. Garrett,* C. Michael Reynolds,* Walter A. Shaw,† Jeff D. Moore,† Dale C. Smith, Jr.,† Anthony A. Ribeiro,* Robert C. Murphy,§ Richard J. Ulevitch, Colleen Fearns,** Donna Reichart,†† Christopher K. Glass,†† Chris Benner,§§ Shankar Subramaniam,§§ Richard Harkewicz,*** Rebecca C. Bowers-Gentry,*** Matthew W. Buczynski,*** Jennifer A. Cooper,*** Raymond A. Deems,*** and Edward A. Dennis[1,***]**

Department of Biochemistry,* Duke University Medical Center, PO Box 3711, Durham, NC; Avanti Polar Lipids, Inc.,† 700 Industrial Park Drive, Alabaster, AL; Department of Pharmacology,§ University of Colorado Health Sciences Center, Mail Stop 8303, PO Box 6508, Aurora, CO; Department of Immunology,** Scripps Institute, La Jolla, CA; Department of Cellular and Molecular Medicine,†† Department of Bioengineering,§§ and Department of Chemistry and Biochemistry and Department of Pharmacology,*** University of California, San Diego, 9500 Gilman Drive, La Jolla, CA

Abstract **The LIPID MAPS Consortium (www.lipidmaps.org) is developing comprehensive procedures for identifying all lipids of the macrophage, following activation by endotoxin. The goal is to quantify temporal and spatial changes in lipids that occur with cellular metabolism and to develop bioinformatic approaches that establish dynamic lipid networks. To achieve these aims, an endotoxin of the highest possible analytical specification is crucial. We now report a large-scale preparation of 3-deoxy-D-*manno*-octulosonic acid $(Kdo)_2$-Lipid A, a nearly homogeneous Re lipopolysaccharide (LPS) sub-structure with endotoxin activity equal to LPS. Kdo_2-Lipid A was extracted from 2 kg cell paste of a heptose-deficient *Escherichia coli* mutant. It was purified by chromatography on silica, DEAE-cellulose, and C18 reverse-phase resin. Structure and purity were evaluated by electrospray ionization/mass spectrometry, liquid chromatography/mass spectrometry and ^{1}H-NMR. Its bioactivity was compared with LPS in RAW 264.7 cells and bone marrow macrophages from wild-type and toll-like receptor 4 (TLR-4)-deficient mice. Cytokine and eicosanoid production, in conjunction with gene expression profiling, were employed as readouts. Kdo_2-Lipid A is comparable to LPS by these criteria. Its activity is reduced by $>10^3$ in cells from TLR-4-deficient mice. The purity of Kdo_2-Lipid A should facilitate structural analysis of complexes with receptors like TLR-4/MD2.**—Raetz, C. R. H., T. A. Garrett, C. M. Reynolds, W. A. Shaw, J. D. Moore, D. C. Smith, Jr., A. A. Ribeiro, R. C. Murphy, R. J. Ulevitch, C. Fearns, D. Reichart, C. K. Glass, C. Benner, S. Subramaniam, R. Harkewicz, R. C. Bower-Gentry, M. W. Buczynski, J. A. Cooper, R. A. Deems, and E. A. Dennis. **Kdo_2-Lipid A of *Escherichia coli*, a defined endotoxin that activates macrophages via TLR-4.** ***J. Lipid Res.*** **2006.** 47: **1097–1111.**

Manuscript received 13 January 2006 and in revised form 7 February 2006.

Published, JLR Papers in Press, February 14, 2006.
DOI 10.1194/jlr.M600027-JLR200

Supplementary key words 3-deoxy-D-*manno*-octulosonic acid-Lipid A • *Escherichia coli* • Re • endotoxin • macrophage • mass spectrometry • LIPID MAPS • toll-like receptor-4

The LIPID MAPS consortium is developing quantitative methods for evaluating the composition, biosynthesis, and function of all macrophage lipids (1). These amphipathic substances not only are structural components of biological membranes but also play important roles in the pathophysiology of inflammation, atherosclerosis, and growth control. Additional lipid functions should emerge from the comprehensive analysis of macrophage lipids. Electrospray ionization/mass spectrometry (ESI/MS) (2, 3), coupled with prefractionation methods like reverse-phase liquid chromatography (LC), is being applied systematically to set the stage for the seamless integration of lipid metabolism into the broader fields of genomics, proteomics, and systems biology. To facilitate this endeavor, LIPID MAPS has introduced a new comprehensive classification system for biological lipids, amenable to computer-based data processing and substructure comparison (4). The eight LIPID MAPS categories are *1*) fatty acyls, *2*) glycerolipids, *3*) glycerophospholipids, *4*) sphingolipids, *5*) sterol lipids, *6*) prenol lipids, *7*) saccharolipids,

Abbreviations: COX-2, cyclo-oxygenase 2; DPBS, Dulbecco's phosphate-buffered saline; ELSD, evaporative light-scattering detection; ESI/MS, electrospray ionization/mass spectrometry; Kdo, 3-deoxy-D-*manno*-octulosonic acid; LC/MS, liquid chromatography/mass spectrometry; LPS, lipopolysaccharide; MRM, multiple-reaction monitoring; Pam3CYS, tripalmitoyl-*S*-glyceryl-cysteine; TBAP, *t*-butyl ammonium phosphate; TLR, toll-like receptor; TNFα, tumor necrosis factor-α; XIC, extracted ion chromatogram.

[1] To whom correspondence should be addressed.
e-mail: edennis@ucsd.edu

and *8*) polyketides. More details are available on the LIPID MAPS web site (www.lipidmaps.org).

As an initial test of the LIPID MAPS approach, the time-dependent response of the macrophage to stimulation by lipopolysaccharide (LPS) is being investigated. LPS is a potent activator of the innate immunity receptor TLR-4/MD2 (5–7). LPS, a saccharolipid glycan according to the new LIPID MAPS classification scheme (4), is present in the outer membranes of most Gram-negative bacteria (6, 8–10). It stimulates macrophages via its lipid anchor, which is termed lipid A (or endotoxin). Animal cells can detect picomolar lipid A concentrations using TLR-4/MD2 and accessory proteins such as CD14 and LPS binding protein (5, 7, 11, 12). Human volunteers injected with 4 ng/kg of LPS develop fever and a flu-like illness, lasting 24 to 48 h (13). Recent clinical studies in humans have characterized the complex response to endotoxin injection by using micro-array technology (14, 15). This approach revealed that the transcription of hundreds of genes is activated or repressed in human leukocytes following exposure to endotoxin (15). Excessive endotoxin exposure during severe Gram-negative sepsis contributes to shock, multiple organ failure, and death. A promising approach to the amelioration of endotoxin-induced illnesses has emerged with the discovery that certain synthetic lipid A analogs (13, 16) or precursors (17) can antagonize the effects of lipid A (endotoxin) on TLR-4/MD2. The former are currently in clinical trials (13, 16).

A limitation of using native LPS from wild-type Gram-negative bacteria for clinical or biological studies of endotoxin activity is its large size and micro-heterogeneity, especially in the length and composition of its terminal glycan chains (6, 9). Direct detection and quantification by mass spectrometry of intact LPS in blood or biological samples is not yet possible. Accordingly, LPS levels are usually estimated by indirect methods, such as the clotting of the amoebocyte limulus lysate induced by the lipid A moiety of LPS (18, 19). The tissue distribution and metabolism of LPS injected into animals have likewise been difficult to evaluate because of the same micro-heterogeneity problem. Knowledge of endotoxin tissue levels and metabolism might suggest new therapeutic approaches to problems of sepsis and inflammation.

We now report the large-scale purification, structural analysis, and biological characterization of a chemically defined LPS, consisting of lipid A and an attached 3-deoxy-D-*manno*-octulosonic acid (Kdo) disaccharide (**Fig. 1**, compound A) (6). This substance, designated Kdo_2-Lipid A, was purified from an *Escherichia coli* K-12 mutant that synthesizes a truncated LPS because of a mutation in the enzymes that normally attach the heptose residues of the LPS core domain (6, 20, 21). This LPS preparation has an intact lipid A anchor, which is fully active as an endotoxin by various biological criteria, such as the stimulation of RAW 264.7 macrophage-like tumor cells to produce eicosanoids and tumor necrosis factor-α (TNFα). Kdo_2-Lipid A is highly selective for TLR-4 and has the distinct advantage that it can be quantified by ESI/MS. The chemical purity of Kdo_2-Lipid A is sufficient to enable high-resolution structural studies, such as NMR spectroscopy or X-ray crystallography of its complexes with important receptor proteins or enzymes (7).

EXPERIMENTAL PROCEDURES

Materials

Tryptone, yeast extract, L-broth, tetracycline, and glucose were obtained from Difco. Chloroform and methanol were purchased from EMS. Cyclohexane was obtained from Burdick and Jackson. EDTA, *t*-butanol, and *t*-butyl ammonium phosphate (TBAP) were from Aldrich. Ammonium acetate and acetonitrile were obtained from Acros. Ethanol, ammonium hydroxide, isopropanol, and sodium chloride were from Fisher Scientific (Fair Lawn, NJ). Silica gel was provided by Grace Davison. Silica gel modified by Astec was used as the C18 reverse-phase resin. Whatman DE 23 DEAE cellulose ion exchange resin and Whatman Partsil K6 TLC plates were purchased from VWR. Lipid visualization after TLC was performed by spraying the plates with 10% H_2SO_4 in ethanol, followed by charring.

RAW 264.7 cells were obtained from the American Type Culture Collection. They were grown for no more than 24 passages on DMEM (Cellgro), supplemented with 10% fetal bovine serum (Hyclone) and 1% penicillin/streptomycin (Invitrogen; Carlsbad, CA). For cell stimulation experiments, the LPS from *E. coli* 0111:B4 was obtained from Sigma (# L4130). Kdo_2-Lipid A was prepared as described below. All liquid chromatography/mass spectrometry (LC/MS) solvents used for prostaglandin analysis were OmniSolv grade or the equivalent from EMD Chemicals (Gibbstown, NJ). The formic acid was purchased from Fisher Scientific. All other fine chemicals were analytical reagent grade or better.

E. coli cell growth conditions

The heptose-deficient *E. coli* mutant WBB06 (20) was grown on a modified Luria-Bertani broth (22). A 500 l capacity IF-500 fermentor was filled with 375 l of water, containing 3,750 g of tryptone (10 g/l), 1,875 g yeast extract (5 g/l), 3,750 g NaCl (10 g/l), and 750 g glucose (2 g/l). After sterilization, 4.5 g of tetracycline (12 mg/l) was added from a concentrated filter-sterilized stock solution in 70% aqueous ethanol. The pH of the growth medium was adjusted to 7.2 with NaOH and H_3PO_4. After 24 h of growth to early stationary phase at 37°C, the WBB06 cells were harvested by centrifugation in a CEPA Z-41 continuous-flow centrifuge. The cell paste (approximately 2 kg) was frozen at −80°C.

Extraction and purification of Kdo_2-Lipid A from *E. coli* WBB06

The overall scheme for the purification is summarized in **Fig. 2**. A modified Folch extraction procedure was used to recover the lipids (23). The frozen WBB06 cells were dispersed in a single-phase solvent mixture consisting of 15 ml chloroform-methanol (2:1; v/v) per gram of cell paste. The suspended paste was stirred overnight at room temperature. The insoluble residue was removed, and the supernatant, containing the extracted lipids, was stored at −20°C. The residue was reextracted overnight at room temperature with 7.5 ml of chloroform-methanol (2:1; v/v) per gram of initial cell paste. The reextracted residue was discarded, and the second supernatant was pooled with the first. The combined supernatants were converted to a two-phase system by adding 20% of their total volume as aqueous 1.0 M NaCl. The lower organic phase was recovered, and the solvent was removed by rotary evaporation. The weight of the extracted lipids, which consist mainly of phosphatidyl-

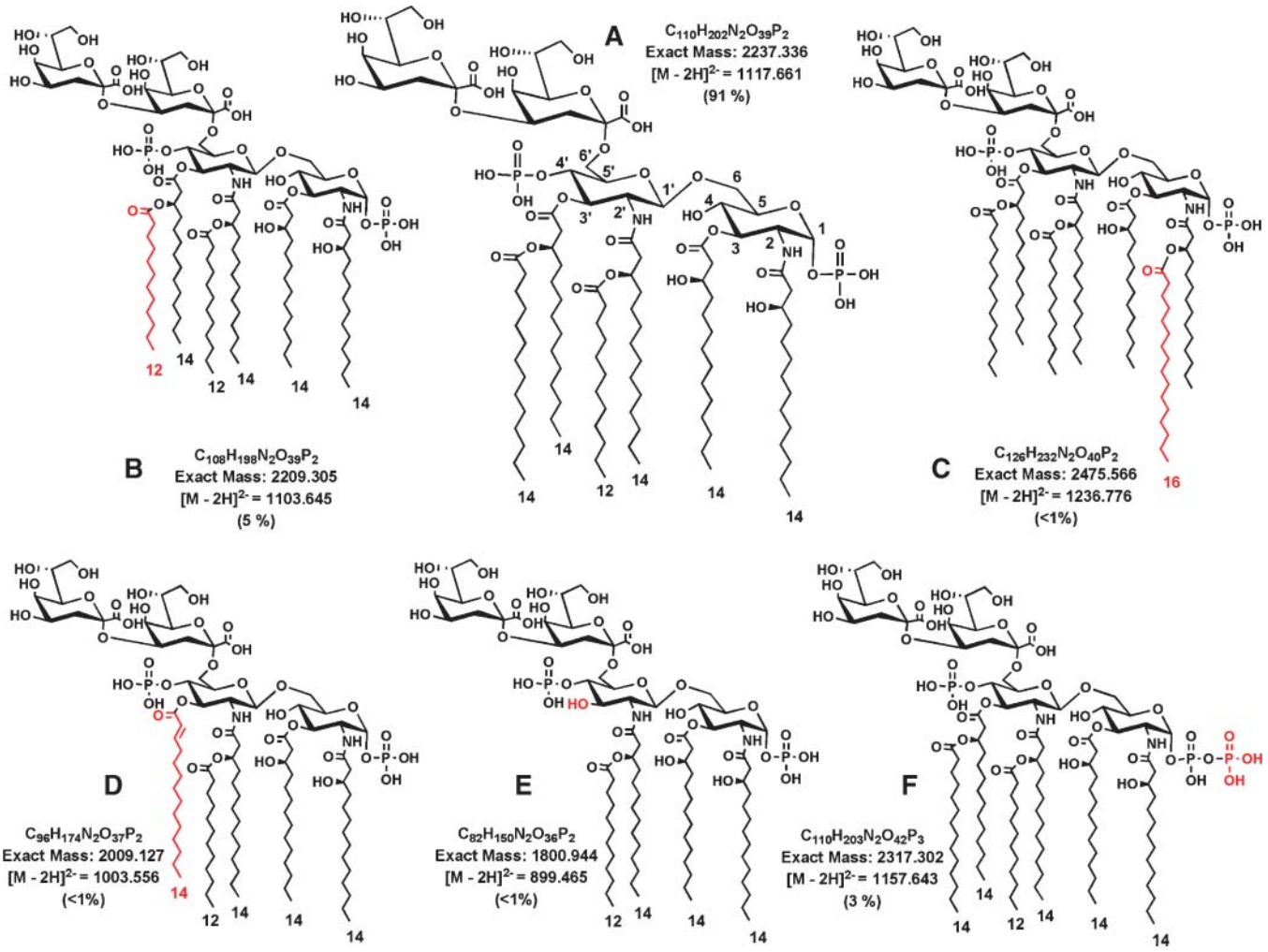

Fig. 1. Structure of 3-deoxy-D-*manno*-octulosonic acid $(Kdo)_2$-Lipid A and related minor lipids purified from *Escherichia coli* WBB06. This mutant is defective in the WaaC and WaaF glycosyltransferases that attach heptose to the lipopolysaccharide (LPS) core (6). Therefore, about two-thirds of the lipid A made by WBB06 is compound A, and the rest is mostly its 1-diphosphate derivative (44, 47), compound F. Following purification, compound A represents ~91%, compound B ~5%, and compound F ~3% of the total. B and F are expected have the same biological activity as A, given their similar structures (8). B arises in cells because of the lack of acyl chain length selectivity of the LpxM acyltransferase (65, 66). The origin of F is unknown. Other molecular species still present as trace contaminants are compounds C, D, and E, each of which represents less than 1% of the total. The hepta-acylated derivative C arises from A in cells by the action of the PagP acyltransferase (67). Compounds D and E are decomposition products. The numbers of carbon atoms in each acyl chain are indicated. Key structural differences in compounds B through F are highlighted in red.

ethanolamine, phosphatidylglycerol, and Kdo_2-Lipid A, was approximately 65.3 g, or 3.2% of the initial cell paste weight. The extracted lipids were stored neat at −20°C.

The Kdo_2-Lipid A was purified from the WBB06 membrane phospholipids on a normal-phase silica column, consisting of 20 g silica gel per gram total lipid. The silica was prepared by washing with two column volumes of 2% ammonium EDTA in methanol-water (1:1; v/v), followed by extensive washing with methanol-water (1:1; v/v) until the eluant pH was less than 8. The column was then washed with methanol, followed by chloroform. The extracted lipids were dissolved and loaded onto the column in chloroform-methanol (8:2; v/v). The lipids were eluted with a gradient that started at chloroform-methanol-water, 80:20:2 (v/v/v) and ended at 65:35:8 (v/v/v). Fractions containing Kdo_2-Lipid A were identified by TLC (R_f, ~0.3) using the mobile-phase chloroform-methanol-water (65:35:8; v/v/v). The fractions were pooled, and solvent was removed by rotary evaporation. The weight of lipids in the pooled fractions was 9.0 g, or 15% of the total lipid weight loaded onto the column. The Kdo_2-Lipid A was ~70% pure at this stage, as judged by HPLC (see below).

Purification by reverse-phase chromatography was performed as described previously on a C18 column to separate the predominant hexa-acylated Kdo_2-Lipid A (Fig. 1) from minor hepta-, penta- and tetra-acylated lipid A species, and from minor phospholipid contaminants, using a two-solvent mixture. Solvent A is acetonitrile-water (1:1) with 1 mM TBAP, and solvent B consists of isopropanol-water (85:15; v/v) with 1 mM TBAP in water (22). The reverse-phase chromatography column consisted of 60 g of resin per gram of lipid. The pooled fractions, containing the predominant hexa-acylated form of Kdo_2-Lipid A, were extracted with chloroform and aqueous 0.5 M ammonium acetate. Solvent was removed by rotary evaporation, and the lipid was stored neat at −20°C.

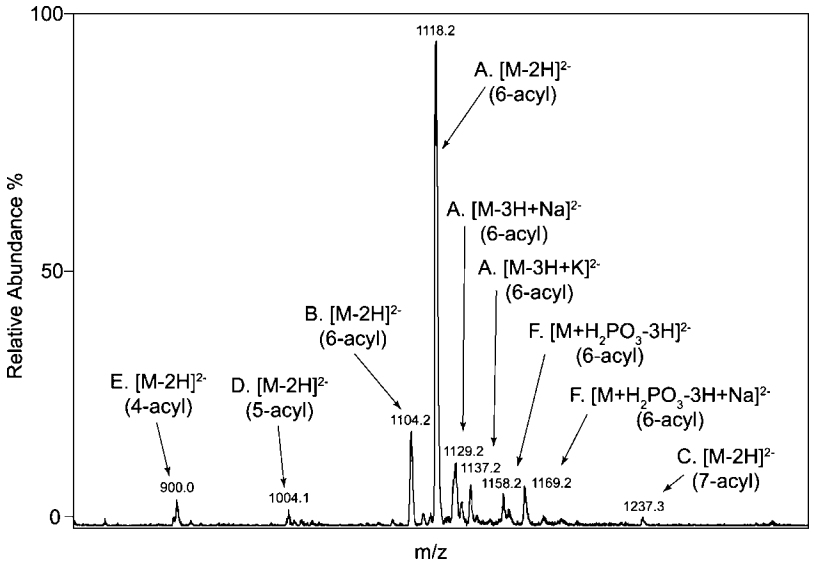

Fig. 2. Electrospray ionization/mass spectrometry (ESI/MS) analysis in the negative mode of purified Kdo_2-Lipid A. The sample at 10 μg/ml in acetonitrlle-water (70:30; v/v) containing 10 mM ammonium acetate was infused at 10 μl/min and scanned in the negative-ion mode in the Q3 of the API 4000 Q Trap® mass spectrometer. Uppercase letters A–F refer to the structures shown in Fig. 1. The *m/z* values for the major isotopic species are indicated.

Removal of TBAP and remaining pigments was accomplished by column chromatography on DEAE-cellulose in the solvent chloroform-methanol-water (2:3:1; v/v/v) with ammonium acetate elution (22). The DEAE-cellulose column consisted of 30 ml DEAE cellulose bed volume per gram of lipid. Pooled fractions containing the Kdo_2-Lipid A were extracted with chloroform and aqueous 0.5 M ammonium acetate. Solvent was removed by rotary evaporation, and the lipids were stored neat at −20°C.

Final purification to remove residual contaminants was achieved with a second normal-phase chromatography column, consisting of 20 g of silica gel per gram of lipid. Kdo_2-Lipid A dissolved in chloroform-methanol was applied to the column, which was eluted as described above. Solvent was removed by rotary evaporation from the final pooled fractions containing the Kdo_2-Lipid A. The residue was reconstituted in cyclohexane-*t*-butanol (1:1;v/v) and freeze dried. The final overall yield obtained by this procedure was 1.4 g of hexa-acylated Kdo_2-Lipid A as the ammonium salt (>95% pure by HPLC). Long-term storage at −16°C to −24°C is recommended.

The Kdo_2-Lipid A in the ampoules was prepared for use in cell stimulation experiments by dispersing it in sterile Dulbecco's phosphate-buffered saline (DPBS) at 1 mg/ml by sonic irradiation in a bath sonicator for 5 min. A 100 μl portion of this stock was then diluted with 900 μl sterile DPBS. This 100 μg/ml (1,000×) aqueous dispersion of Kdo_2-Lipid A was subjected to a second sonic irradiation prior to being added to the cells to yield a final concentration of 100 ng/ml in the growth medium.

HPLC analysis of Kdo_2-Lipid A

HPLC analysis of Kdo_2-Lipid A was performed using an Agilent 1100 quaternary pump system, equipped with a temperature-controlled column compartment and an in-line solvent degassing unit. The Zorbax Eclipse XDB-C8 column (150 mm × 4.6 mm, 5 μ particle size) (Agilent Technologies; Palo Alto, CA) was maintained at 40°C. Samples were eluted using a gradient that consisted of methanol-water-chloroform (62:36:2; v/v/v) with 10 mM ammonium acetate as mobile-phase A and chloroform-methanol-water (80:20:2; v/v/v) with 50 mM ammonium acetate as mobile-phase B. The flow rate was 1 ml/min. Chemicals and solvents were HPLC grade and purchased from Fisher Scientific. The initial solvent, consisting of 85% A and 15% B, was maintained for 2 min, followed by a linear gradient to a final composition of 70% A and 30% B after 20 min; the solvent was held at the same composition until 30 min. A 10 min reequilibration of the column with 85% A and 15% B was performed prior to the next injection.

The material eluting from the column was directed to a SEDEX model 75C evaporative light-scattering detector (S.E.D.E.R.E., France). Zero-grade compressed air was used to nebulize the postcolumn flow stream at 3.5 bar into the detector at 50°C, set at a photomultiplier gain of 6. The detector signal was transferred to the Agilent HPLC Chemstation software for integration. The Kdo_2-Lipid A samples were prepared at 1 mg/ml in a mixture of 85% A and 15% B (as defined above). Ten micrograms was injected onto the column for purity assessment by HPLC and evaporative light-scattering detection (ELSD).

Mass spectrometry of Kdo_2-Lipid A and eicosanoids

Flow injection analysis of Kdo_2-Lipid A was carried out using an ABI 4000 Q Trap® tandem quadrupole mass spectrometer (Applied Biosystems; Thornhill, Ontario, Canada) with negative-ion electrospray ionization during infusion of 10 μl/min of acetonitrile-water (70:30; v/v) containing 10 mM of ammonium acetate. The electrospray voltage was set at −4.5 kV, and nitrogen was used as curtain gas. LC/MS and low-resolution LC/MS/MS were carried out using a reverse-phase C8 HPLC column (Agilent), operated at a flow rate of 1 ml/min under gradient conditions, as described above. At this flow rate, the turbo ion spray interface was set at 600°C. For MS/MS experiments, nitrogen was used as collision gas at a collision energy of −15 V (laboratory frame of reference).

High-resolution electrospray mass spectrometry was carried out using a tandem hybrid quadrupole time-of-flight mass spectrometer (ABI Qstar XL, Applied Biosystems) by infusion of 50 ng/μl Kdo_2-Lipid A in chloroform-methanol (2:1; v/v) at 6 μl/min. The instrument was scanned from *m/z* 100–2,500 in a negative-ion mode with the electrospray set at −4.2 kV. Nitrogen was used as collision gas and collisional activation of ions was performed at −40.0 V (laboratory frame of reference). This instrument was calibrated using polypropylene glycol 300 (Applied Biosystems) and had an average mass accuracy of 10–20 ppm.

The quantitative analysis of eicosanoids was carried out by LC/MS/MS using a tandem quadrupole mass spectrometer (ABI 4000 Q Trap®, Applied Biosystems), using stable isotope dilution and the multiple-reaction monitoring (MRM) mode. For each

sample, a deuterium-labeled internal standard consisting of d_4-PGE_2 (99 atom % d_4; Cayman Chemical, Ann Arbor, MI) was added to the cell supernatant just prior to sample workup. Cellular debris was removed by centrifugation (3,000 *g*, 10 min). Methanol and acetic acid were added to a final concentration of 10% and 2%, respectively. Eicosanoids were extracted using solid-phase extraction columns (Strata-X; Phenomenex, Rockville, IL). These columns were preconditioned by washing with 2 ml methanol, followed by 2 ml water. The sample was then loaded, and the column washed with 2 ml 0.5% methanol. The eicosanoids were eluted from the column using 1 ml of methanol. This eluate was dried under vacuum and redissolved in 100 μl of solvent system C [water-acetonitrile-formic acid (63:37:0.02; v/v/v)]. Standard curves were prepared in separate experiments in order to relate the abundance of MRM transitions to that of the deuterium-labeled internal standard (10 ng), using primary standards of each eicosanoid (Cayman Chemical).

Eicosanoids were separated by reverse-phase HPLC on a reverse-phase C18 column (2.1 mm × 250 mm; Grace-Vydac, Hesperia, CA) operated at a flow rate of 300 μl/min at 25°C. The column was initially equilibrated with 100% solvent C. Samples were then loaded through a 5 μl injection loop and eluted with a linear gradient from 0%–20% solvent D, consisting of acetonitrile-isopropanol (1:1; v/v), in 6 min; next, solvent D was increased to 55% in 6.5 min, and held until 10 min. Finally, solvent system D was linearly increased to 100% in 2 min and held for an additional 1 min. In order to recycle the column, the solvent system was switched to 100% C at 13.5 min and held until 16 min. The mass spectrometer was run in the MRM mode with the electrospray ion source operating in the negative mode (−4.5 kV), with the turbo ion spray source set at 525°C. Collisional activation of each of the eicosanoid precursor ions was carried out using nitrogen as collision gas. Specific MRM pairs are as follows: 11β-$PGF_2\alpha$ and $PGF_2\alpha$ at *m/z* 353 → 193 (−80 V); PGE_2 and PDG_2 at *m/z* 351 → 189 (−50 V); PGJ_2 at *m/z* 333 → 189 (−30 V); 15D-PGD_2 at *m/z* 333 → 271 (−30 V); 15D-PGJ_2 at *m/z* 315 → 271 (−108 V); and 11-HETE at *m/z* 319 → 167 (−30 V). The deuterium-labeled internal standards (d_4-PGE_2 and d_4-PGD_2) were monitored at *m/z* 355 → 193. In some cases, the same MRM pairs were used to monitor different eicosanoids (i.e., PGE_2 and PGD_2); however, because these eluted at different HPLC retention times, they can be analyzed independently.

NMR spectroscopy of Kdo_2-Lipid A

For NMR analysis, a 1 mg sample of Kdo_2-Lipid A was dissolved in 0.3 ml $CDCl_3$-CD_3OD-D_2O (2:3:1; v/v/v) and analyzed by ^{1}H-COSY, TOCSY, and NOESY at 600 MHz, as described previously for lipid A and related compounds (24–26). All spectra were recorded at 25°C.

Cell stimulation experiments

RAW 264.7 mouse macrophage tumor cells were plated in DMEM with 10% fetal bovine serum (HyClone Labs; Provo Utah), 100 U/ml penicillin, and 100 μg/ml streptomycin (Invitrogen). The cells were maintained at 37°C in a humidified 5% CO_2 atmosphere. Prior to stimulation, cells were plated at a density of 5×10^5 cells per well in 25 cm^2 flasks and were allowed to adhere for 24 h. They were then washed with PBS and switched to fresh DMEM containing 0.5% fetal bovine serum for another 18 h. Cells were then exposed to either 100 ng/ml LPS (Sigma L4130 from *E. coli* 0111:B4) or 100 ng/ml of Kdo_2-Lipid A for 24 h. Both the LPS and the Kdo_2-Lipid A were suspended in PBS, and the solutions were bath-sonicated before each experiment.

TNF determination

TNFα levels were determined with the mouse TNFα immunoassay kit from R and D Systems, Inc. (Minneapolis, MN), according to the manufacturer's instructions. Typically, 50 μl portions of the cell culture medium were removed from control and treated cells, and frozen at −20°C prior to assay. TNFα levels are expressed as pg/ml or ng/10^6 cells.

TLR-4 selectivity of Kdo_2-Lipid A

Total bone marrow cells were isolated from C57Bl/6 (wild-type) and $TLR4^{-/-}$ mice (27), and then cultured in DMEM supplemented with 10% fetal calf serum, 1% penicillin-streptomycin, and 30% L929 conditioned medium. Cells were seeded at 5×10^5/ml in DMEM, supplemented as above, and allowed to adhere for 2–3 h at 37°C in an atmosphere of 10% CO_2. The cells were then washed with DMEM and supplemented with 10% serum and 1% penicillin-streptomycin, prior to 24 h stimulation with the indicated concentrations of Kdo_2-Lipid A or the TLR2 ligand tripalmitoyl-*S*-glyceryl-cysteine (Pam3CYS). The concentrations of IL-6 in the culture supernatants were measured by ELISA, using reagents purchased from Pharmingen. The $TLR4^{-/-}$ mice were obtained from Dr. S. Akira (27, 28).

Microarray comparison of Kdo_2-Lipid A and LPS

RAW 264.7 mouse macrophage tumor cells were treated with 100 ng/ml LPS or Kdo_2-Lipid A, prepared as described above, for 6 h. Total RNA was purified using RNeasy columns (Qiagen).

RNA analysis by Northern blotting was performed as described previously (29). Ten micrograms total RNA were separated by gel electrophoresis and transferred to nylon (Supercharge, Scheicher and Schuell). Prior to hybridization, membranes were cross-linked by UV treatment (Stratagene) and stained with Methylene Blue (Molecular Research Center, Cincinnati, OH). COX-2 and GAPDH probes (30) were generated by RT-PCR, followed by random prime labeling (Amersham Biosciences) and hybridization with QuikHyb (Stratagene). Microarray experiments were performed using the Codelink Uniset 1 mouse microarray platform (Amersham), according to the manufacturer's directions.

RESULTS

Extraction and purification of Kdo_2-Lipid A from *E. coli* WBB06

A modified Folch extraction (23) was used to recover the lipids from the cell paste. The total lipid extract was fractionated by normal-phase silica chromatography, yielding a mixture of major and minor Kdo_2-Lipid A species (Fig. 1). The purity at this stage was estimated by HPLC to be ~70% hexa-acylated Kdo_2-Lipid A. Subsequent separation of the hexa-acylated material from the other molecular species was achieved by reverse-phase chromatography, followed by DEAE cellulose chromatography to remove TBAP and remaining pigments (22). This step yielded the ammonium salt of Kdo_2-Lipid A. Finally, a second normal-phase silica chromatography was used to remove residues carried over from the reverse-phase and DEAE resins. The overall yield from 2 kg of cell paste was 1.4 g of the ammonium salt of hexa-acylated Kdo_2-Lipid A.

ESI/MS and HPLC analysis of purified Kdo_2-Lipid A

A 1 mg/ml sample of the purified material was dissolved in chloroform-methanol-water (80:20:2; v/v/v), further diluted to 10 μg/ml with acetonitrile-water (70:30: v/v) containing 10 mM ammonium acetate, and infused into an ABI 4000 Q Trap® mass spectrometer at a flow rate of 10 μl/min. The mass range of *m/z* 500–1,400 was scanned in the negative-ion mode (Fig. 2). The most prominent species were interpreted as the $[M\text{-}2H]^{2-}$ ions of the hexa-acylated compounds A and B (Fig. 1) at *m/z* 1,118.2 and 1,104.2, respectively. These substances differ in the lengths of their 3′ secondary acyl chains, which are C14 for A and C12 for B (Fig. 1). Sodium and potassium addition adducts of A were observed at *m/z* 1,129.2 and 1,137.2, respectively. Minor impurities were seen at *m/z* 1,237.3 (compound C), *m/z* 1,004.2 (compound D), *m/z* 900.0 (compound E), and *m/z* 1,158.2 and 1,168.2 (compound F). The masses of labeled peaks shown in Fig. 2 represent the most abundant isotopic forms of each compound (Fig. 1), which are ~1 amu larger than the exact masses due to the more abundant M+1 isotope (data not shown).

The Kdo_2-Lipid A preparation was further evaluated for purity by HPLC/ELSD. A 10 μg sample was injected onto a reverse-phase column, as described above. The peak areas determined by this analysis more closely reflect the mole ratios of the various components than do the peak intensities observed by mass spectrometry (Fig. 2). However, neither method is quantitative when implemented without standards. The major peak at 21.45 min in the HPLC/ELSD experiment (**Fig. 3A**), representing compounds A and F (Fig. 1), was ~94% of the total integrated area. The smaller peak at 20.97 min (Fig. 3A) is due to compound B, which is slightly less hydrophobic because laurate replaces a myristate chain in the left glucosamine unit of B (Fig. 1). The combined hexa-acylated species (i.e., compounds A, B, and F) represent 99.1% of the total area in the HPLC/ELSD analysis.

In a separate experiment, the LC system (Fig. 3A) was coupled to the mass spectrometer, and the effluent was scanned in the range of *m/z* 800–1,400 amu. The peaks detected in the direct infusion experiment (Fig. 2) were extracted from the total ion current with a mass offset of ±2 amu to cover the signals arising from all isotopic forms. In this case, a 1 μg sample was injected onto the column. The extracted ion chromatograms (XICs) for the major and minor peaks seen in Fig. 2 were overlaid in Fig. 3B to assess their order of elution in relation to the HPLC/ELSD analysis. The retention times for the compounds were comparable. Compound E (XIC = 899) elutes at 13.76 min, compound D (XIC = 1,004) at 19.18 min, compound B (XIC = 1,004) at 20.43 min, compound A (XIC = 1,118) at 20.78 min, and compound C (XIC = 1,237) at 23.49 min. Compound F (Fig. 1), which is the 1-diphosphate derivative of compound A (XIC = 1,158 for $[M\text{-}2H]^{2-}$), coeluted with compound A at an approximate abundance of 2.8% relative to compound A (data not shown). This order of elution is consistent with the relative hydrophobicity of these substances (Fig. 1). Again, the relative intensity of each extracted ion peak cannot be correlated quantitatively to the relative molar abundance of each lipid species without the use of appropriate standards.

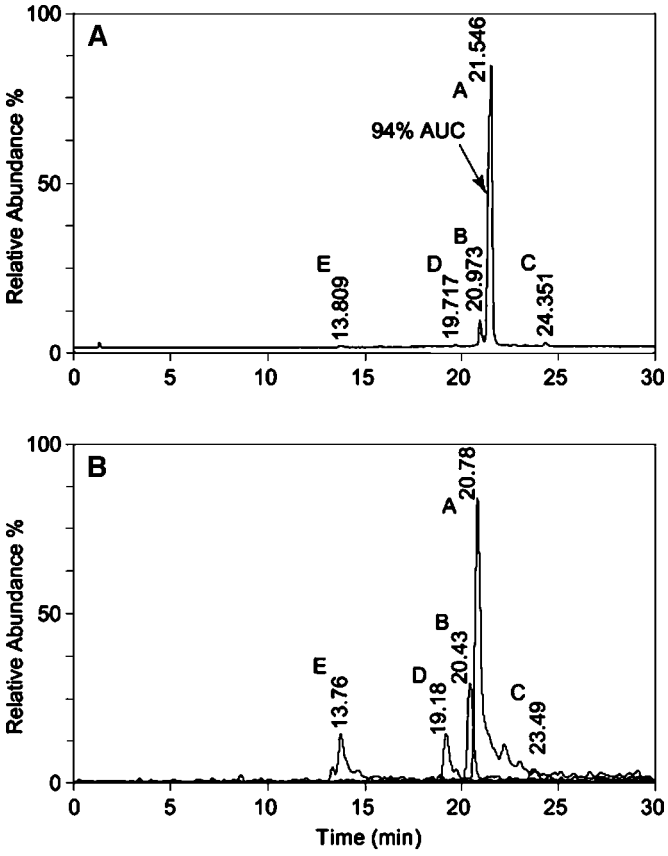

Fig. 3. HPLC/evaporative light-scattering detection and liquid chromatography/mass spectrometry (LC/MS) analysis of purified Kdo_2-Lipid A. A 10 μg sample injected onto a C8 reverse-phase column (A) shows a major component accounting for ~94% of the total. This material corresponds to compound A and small amounts of F (as shown in Fig. 1). The chromatography was optimized with the sample dissolved in solvents A and B of the mobile phases (85:15; v/v). Other more or less polar combinations of these solvents resulted in sample precipitation on the column, peak splitting, poor resolution, and/or reduced sensitivity. Column loads above 50 μg resulted in peak broadening and splitting. Uppercase letters refer to the structures shown in Fig. 1. B: A 1 μg sample was injected onto a C8 reverse-phase column. Each tracing is the extracted ion chromatogram (XIC) from a scan of *m/z* 800–1,400 amu. Compound E (XIC = 899), 13.76 min; compound D (XIC = 1,104), 19.18 min; compound B (XIC = 1,004), 20.43 min; compound A (XIC = 1,118), 20.78 min; and compound C (XIC = 1,237), 23.49 min. Compound F (XIC = 1,158) elutes with compound A.

High-resolution ESI/MS, ESI/MS/MS, and ^{1}H-NMR analysis

A high-resolution quadrupole time-of-flight tandem mass spectrometer (QSTAR®XL; Applied Biosystems) was used to evaluate the exact mass and collision-induced ion fragmentation pattern of the purified Kdo_2-Lipid A. Consistent with the LC/MS and HPLC/ELSD analyses shown above, the predominant ions corresponded to a

hexa-acylated Kdo_2-Lipid A (Fig. 1, compound A). Under these conditions, the Kdo_2-Lipid A forms both doubly and triply charged species, as judged by negative-ion ESI/MS. **Figure 4A** shows the region of the spectrum corresponding to the major cluster of doubly charged ions derived from natural product, overlaid with the predicted isotopic distribution for a molecule with the molecular formula of compound A in Fig. 1 (predicted monoisotopic $[M\text{-}2H]^{2-}$ at m/z = 1,117.66). The observed m/z at 1,117.66 and the isotopic distribution match the predicted values exactly (Fig. 4A).

To analyze the structure in more detail, the doubly charged Kdo_2-Lipid A ion (m/z =1,117.7) was subjected to collision-induced decomposition mass spectrometry. The resulting MS/MS spectrum is shown in Fig. 4B. All product ions in the MS/MS spectrum are consistent with the structure proposed for compound A in Fig. 1. The Kdo sugars are readily lost from the molecular ion, giving rise to the two major product ions at m/z 219.04 and 439.09. Lipid product ions corresponding to the loss of one or both Kdo residues are also observed. Loss of the Kdo disaccharide yields the doubly and singly charged product ions at m/z 897.6 and 1,796.16, respectively. Loss of one Kdo unit yields a doubly charged product ion at m/z 1,007.6. In addition to the loss of Kdo disaccharide, the neutral loss of the secondary myristate chain was observed, both as singly or

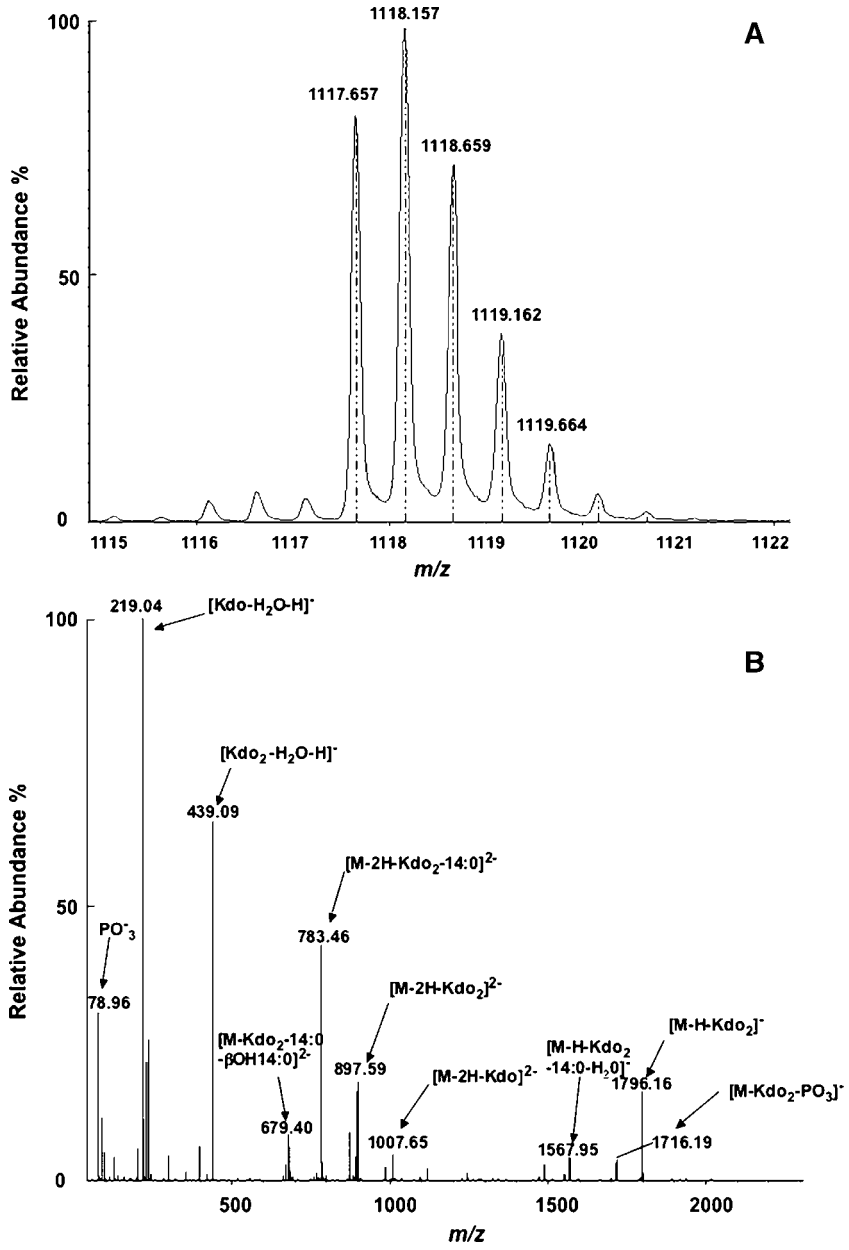

Fig. 4. High-resolution ESI/MS and tandem ESI/MS/MS of the major hexa-acylated Kdo_2-Lipid A molecular species. A: Simulation of the predicted peaks $[M\text{-}2H]^{2-}$ attributed to the major form of Kdo_2-Lipid A (compound A in Fig 1). B: MS/MS analysis of m/z 1,117.7. For all labeled peaks, only the monoisotopic mass is given.

doubly charged product ions at *m/z* 1,567.95 and 783.46, respectively. A more complete interpretation of the ESI/MS/MS spectrum of the Kdo_2-Lipid A and its minor impurities is available on the LIPID MAPS website (www.lipidmaps.org) and should serve as a reference for the analysis of the structures of other lipid A preparations.

The 2D ^1H-^1H COSY of our Kdo_2-Lipid A is shown in **Fig. 5**. It is consistent with previous in-depth studies of related saccharolipid molecules (24–26). The major features of the spectrum are in accord with a hexa-acylated disaccharide of glucosamine, containing two acyloxyacyl groups (24–26) and two Kdo residues (31). Although many of the protons of the Kdo units are not resolved from each other, the spectrum nevertheless supports the proposed structure shown in Fig. 1A. The connectivity of the glucosamine ring protons is indicated in Fig. 5. The NMR analysis gives no evidence for other impurities that might have been overlooked by HPLC and ESI/MS.

LC/MS analysis of eicosanoids from stimulated RAW cells

In the course of setting up the LC/MS system for the comprehensive analysis of eicosanoids in mouse macrophages, we have established a library that includes chromatographic retention times and tandem mass spectrometry data for the most common eicosanoids. To date, this includes over 70 compounds, and we are aggressively updating and expanding its contents. This library is available to the scientific community on the website www.lipidmaps.org. The web visitor can obtain chemical structures for standards in both GIF and ChemDraw® formats, specific details regarding LC and MS parameters employed in our analysis, fragmentation spectra and structures of dominant fragment ions (including literature references, when available, for fragment assignments), and retention times for a stated set of chromatographic conditions. Finally, a web link to Cayman Chemical provides useful information and references on specific eicosanoids.

We have employed this procedure to compare the stimulation of RAW cells with both LPS or Kdo_2-Lipid A. Addition of either ligand yielded the same eicosanoid profile (**Fig. 6**). The major eicosanoid produced was PGD_2 (130 ng/10^6 cells). $PGF_{2\alpha}$ and PGE_2 were also present, but only at 2–5 ng/10^6 cells. In addition, significant amounts of the PGD_2 breakdown products 11β-$PGF_{2\alpha}$, PGJ_2, 15 deoxy PGD_2, and 15 deoxy PGJ_2 were detected (3–15 ng/10^6 cells). Trace amounts (less than 1 ng/10^6 cells) of 11 HETE and arachidonic acid were also routinely detected. The 11 HETE was found to be the 11 (R) HETE, as determined by chiral HPLC, demonstrating that it is a product of a COX enzyme rather than 5-lipoxygenase. In fact, significant levels of 5-lipoxygenase-derived products were not detected with this stimulation protocol. The baseline for eicosanoid production in untreated cells is zero.

We next determined the dose response of the RAW cells to these two ligands. For these studies, we report only the

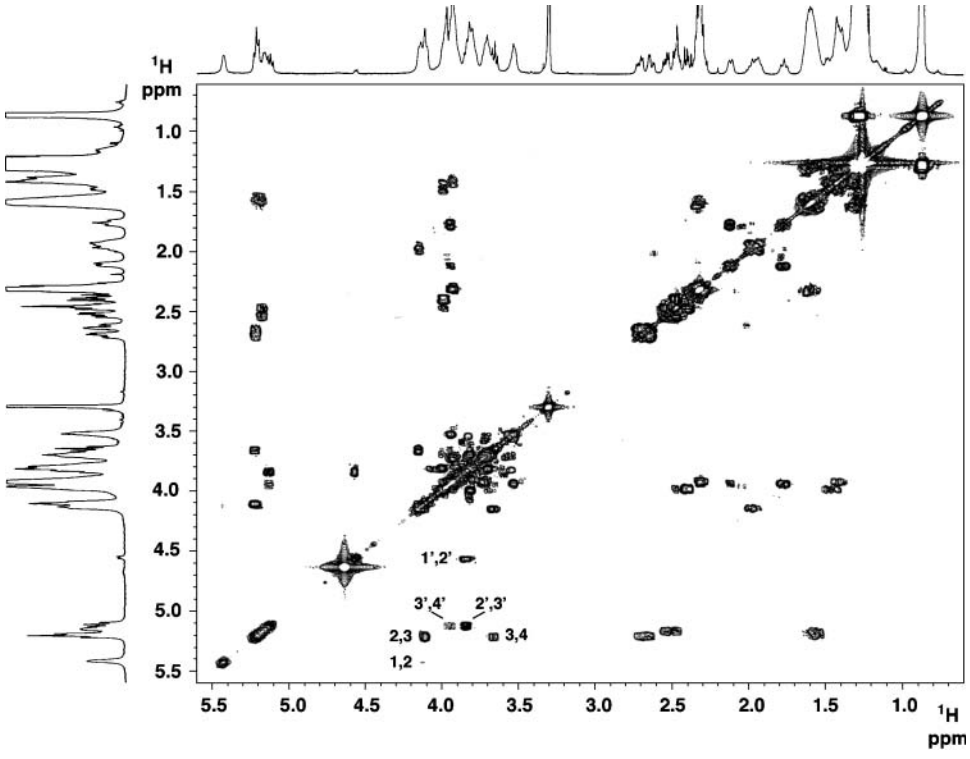

Fig. 5. ^1H-NMR COSY of Kdo_2-Lipid A purified from WBB06. Diagnostic cross-peaks arising from proton-proton couplings in the proximal and distal glucosamine residues are labeled according to the scheme shown in Fig. 1. The spectrum is in accord with previous studies of lipid A NMR spectra (24–26). The characteristic signals between 1.7 and 2.2 ppm arise from the geminal protons at position 3 in the two Kdo units (31).

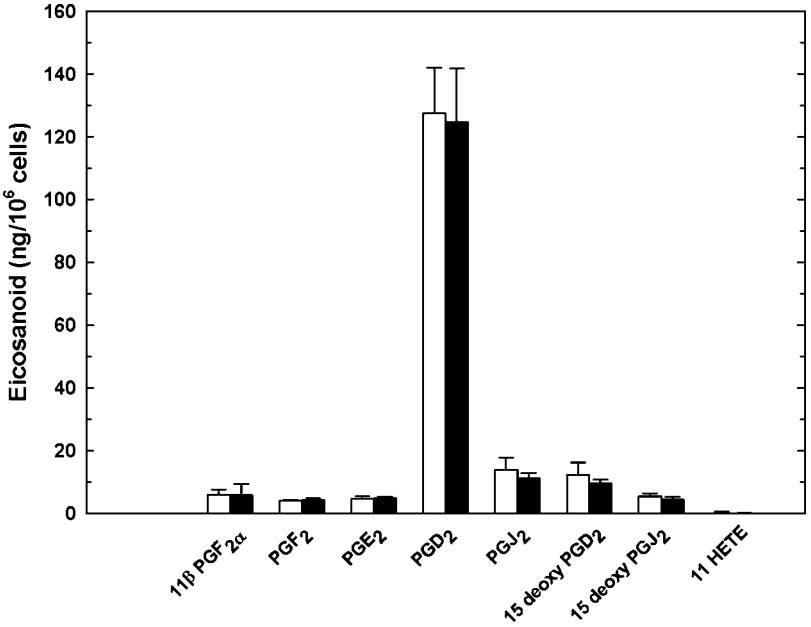

Fig. 6. Profile of prostaglandin production in Kdo_2-Lipid A-stimulated RAW cells. RAW 264.7 cells were stimulated with 100 ng/ml of either LPS (open bars) or Kdo_2-Lipid A (solid bars) for 24 h, as outlined in Experimental Procedures, and the eicosanoid levels were determined by LC/MS/MS. The LPS is very heterogeneous, and its average molecular weight is on the order of 10,000 Da. Error bars represent standard deviation of triplicate measurements.

values for PGE_2 and PGD_2, and the cytokine TNFα, but all of the compounds identified in Fig. 6, within error, followed the same general pattern. **Figure 7** clearly shows that RAW cells exhibit similar responses to LPS or Kdo_2-Lipid A for PGE_2, PGD_2, and TNFα. The maximum responses elicited for each type of saccharolipid were usually within experimental error. For the eicosanoids, the EC_{50} for the LPS was slightly higher than for Kdo_2-Lipid A, perhaps because of the greater purity and smaller molecular mass of Kdo_2-Lipid A. Taking PGD_2 as an example, the EC_{50} for LPS was 79 ± 11 ng/ml, whereas for Kdo_2-Lipid A, it was 11 ± 1 ng/ml. Unlike the eicosanoids, the EC_{50}s for the TNFα response for each saccharolipid were within experimental error, i.e., LPS was 204 ± 22 ng/ml and Kdo_2-Lipid A was 140 ± 70 ng/ml.

The time courses of stimulation are shown in **Fig. 8**. The cells were exposed to either LPS or Kdo_2-Lipid A, as indicated. After 30 min exposure to either ligand, the eicosanoid levels in the media were unchanged from the control levels. By 2 h, there was a 10-fold increase in the eicosanoids in the media from cells stimulated by either ligand. At 24 h, the fold activation of eicosanoid production over controls varied between 500 and several thousand. The TNFα response started sooner than that of the eicosanoids; the levels of TNFα at 2 h were often 1,000-fold higher than at 30 min. The maximum level reached at 24 h was 5,000-fold higher than at 30 min for LPS. The maximum response to LPS stimulation was usually 1.5 to 2 times that for Kdo_2-Lipid A stimulation.

The data presented here represent typical results obtained from at least three experiments carried out on different days and employing cells at different passages. All data points represent the average of at least triplicates run on the same day.

TLR-4 selectivity

As shown in **Fig. 9**, bone marrow macrophages from wild-type mice responded fully to 10 ng/ml Kdo_2-Lipid A, whereas $TLR4^{-/-}$ macrophages did not. In fact, there was no measurable response above the buffer control in the $TLR4^{-/-}$ cells at 100 ng/ml Kdo_2-Lipid A. Only at 1 μg/ml Kdo_2-Lipid A was there a small response in the $TLR4^{-/-}$ cells, suggesting the presence of small amounts of a TLR2-activating contaminant, possibly a bacterial lipopeptide. Both the wild-type and the $TLR4^{-/-}$ bone marrow-derived macrophages also responded vigorously to a synthetic Pam3CYS standard, a well-characterized TLR2 ligand (data not shown) (28).

Microarray analysis

To investigate the relative biological activities of LPS and Kdo_2-Lipid A at the level of global gene expression, experiments were performed comparing the responses of RAW 264.7 cells to both agonists. Engagement of the TLR4 receptor results in the upregulation of hundreds of genes secondary to activation of numerous transcription factors, including NF-κB, AP-1, and IRF3 (28). RAW 264.7 cells were treated for 6 h with 100 ng/ml Kdo_2-Lipid A, 100 ng/ml LPS, or control buffer. The total RNA was extracted and then analyzed on microarrays representing approximately 10,000 independent transcripts. The patterns of inducible genes following LPS or Kdo_2-Lipid A treatment were highly concordant, as illustrated for the 200 most highly inducible LPS target genes (**Fig. 10**).

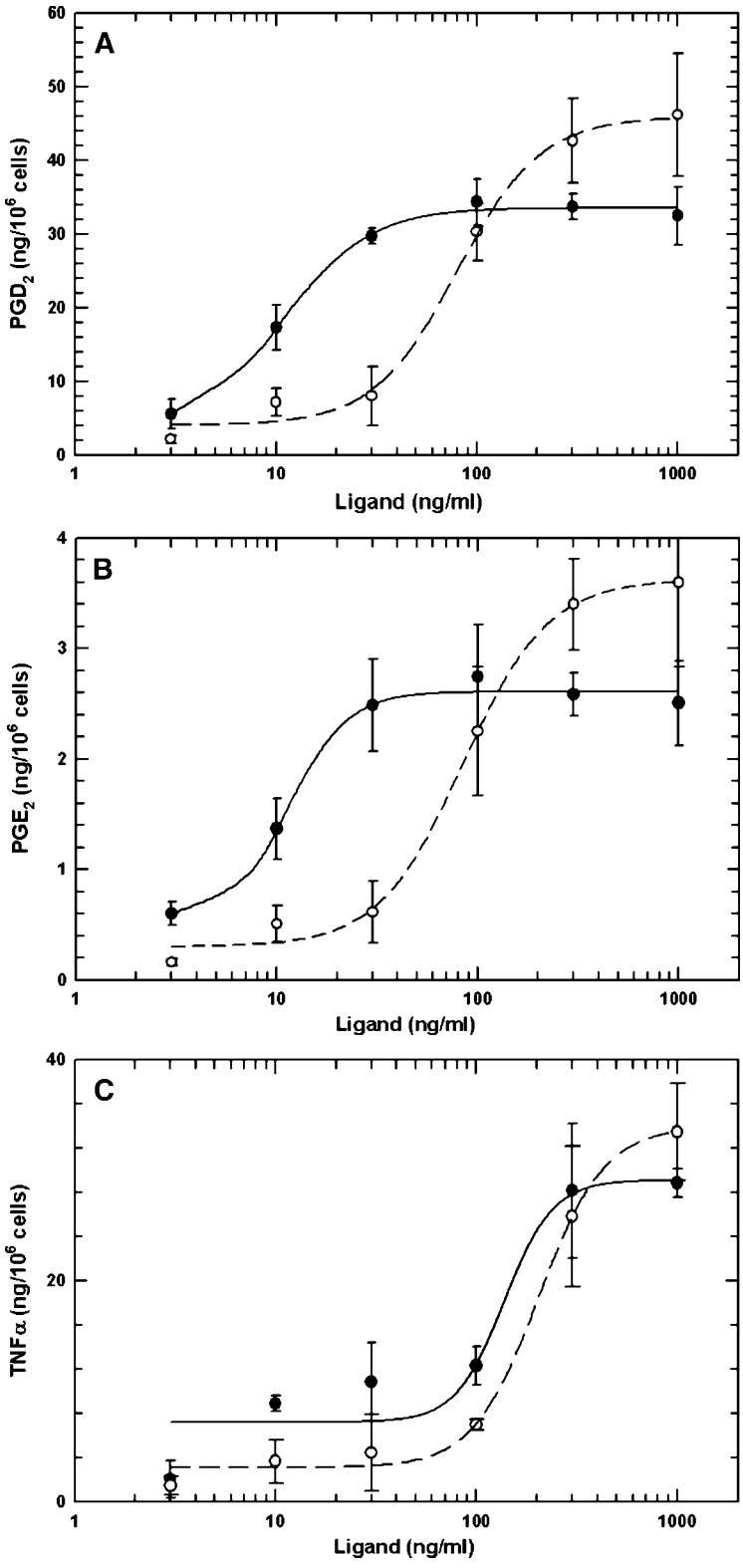

Fig. 7. Dose response curves for Kdo_2-Lipid A- or LPS-stimulated RAW cells. RAW 264.7 cells were stimulated for 24 h with either Kdo_2-Lipid A (closed circles) or LPS (open circles), following the protocol outlined in Experimental Procedures. The release of PGD_2 is shown in panel A, and that of PGE_2 is shown in panel B. Panel C shows the release of tumor necrosis factor-α (TNFα). The lines were obtained by nonlinear regression analysis fitting the data to a four-parameter logistic equation based on a simple binding model (SigmaPlot 9.0, Systat Software, Point Richmond, CA). Error bars represent standard deviation of triplicate measurements.

These results were confirmed for the COX2 gene by Northern blotting (Fig. 10, inset). There were no examples of genes that were highly induced by Kdo_2-Lipid A (i.e., >3-fold) but not induced by LPS. Only one gene in the top 200 genes that were highly induced by LPS was not induced by Kdo_2-Lipid A. This gene corresponds to Mad, a transcription factor that operates as a negative regulator of Myc-dependent transcription (32). Its induction by LPS but not Kdo_2-Lipid A in these studies may be due to contaminants in the LPS preparation that regulate gene expression by TLR4-independent mechanisms. These findings indicate that Kdo_2-Lipid A is a func-

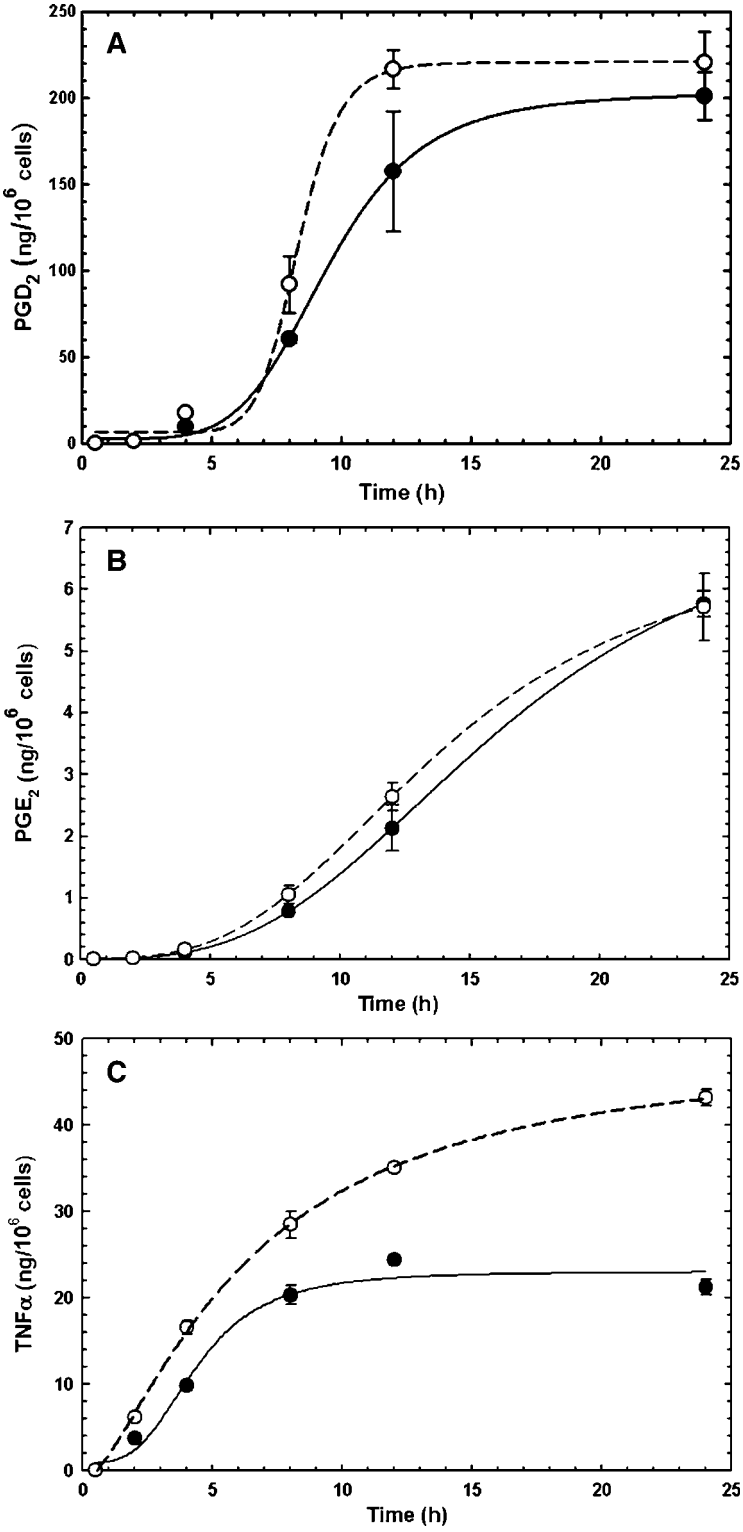

Fig. 8. Time course of eicosanoid release following stimulation of RAW cells with either Kdo_2-Lipid A or LPS. The RAW 264.7 cells were stimulated with 100 ng/ml of either Kdo_2-Lipid A (closed circles) or LPS (open circles), as outlined in Experimental Procedures, with the exception that the exposure to ligand was varied from 0 to 24 h. The release of PGD_2 is shown in panel A, that of PGE_2 is shown in panel B, and that of TNFα is shown in panel C. The lines are best fits to the data points, but do not represent theoretical fits to any particular model. Error bars represent standard deviation of triplicate measurements.

tional mimetic of LPS at the level of gene expression for broad sets of TLR4-sensitive genes.

DISCUSSION

The identification of the toll receptors of the mammalian innate immune system (5, 12, 27, 28, 33) has intensified the search for chemically defined ligands to enable structural and mechanistic studies. The lipid A (endotoxin) moiety of enterobacterial LPS (6, 8) is a potent activator of TLR-4 (5, 12, 27, 28, 33), but well-characterized synthetic or natural lipid A preparations are not generally available. Most studies of TLR-4 activation, including the recent comprehensive characterization of gene expression in humans following endotoxin infusion

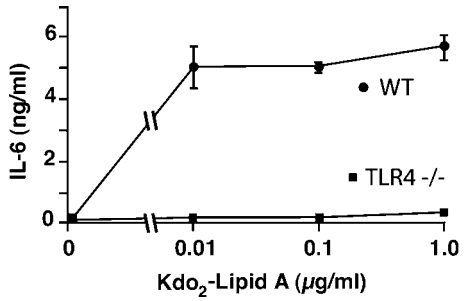

Fig. 9. Toll-like receptor-4 selectivity of purified Kdo_2-Lipid A in mouse bone marrow macrophages. WT, wild type. Error bars represent standard deviation.

(15), have relied on crude LPS preparations, which are obtained from Gram-negative bacteria by phenol extraction and phase partitioning (34, 35). The extensive microheterogeneity of both the lipid and carbohydrate portions of commercial LPS is well documented (9). Furthermore, most intact LPS preparations have not been characterized by mass spectrometry or NMR spectroscopy, primarily because of their heterogeneity, large size, and insolubility (9, 36, 37). It is therefore not surprising that different commercial LPS preparations can vary widely in their biological activities.

Chemical syntheses of pure lipid A molecular species (the endotoxin component of LPS) and of various lipid A analogs have been reported (16, 38–41). The most relevant of these compounds, such as *E. coli* lipid A 38, are not easy to prepare and are not readily available to the scientific community. Kdo_2-Lipid A represents an even greater synthetic challenge than lipid A per se (39). To date, its synthesis has been reported by only one group of investigators (39). This situation may change with the development of automated carbohydrate synthesizers (42, 43). However, the addition of phosphate groups and acyl chains to the glucosamine disaccharide backbone of lipid A presents special technical problems, and the glycosidic linkages formed by Kdo are relatively unstable in the presence of mild acid (44). Chemo-enzymatic approaches, using synthetic lipid A in conjunction with recombinant, purified Kdo transferase, may offer the best long-term solution for the future. However, at the present time, the preparation of lipid A and related molecules from large-scale fermentations of selected Gram-negative bacteria remains the best option.

As part of the systematic LIPID MAPS effort to quantify all macrophage lipids in response to endotoxin stimulation, we have developed a new large-scale purification of Kdo_2-Lipid A (Fig. 1, compound A), a substructure of LPS made by heptose-deficient mutants of *E. coli* (6). This material can be extracted from cells with chloroform-methanol mixtures, like a glycerophospholipid, i.e., without the use of phenol or mild-acid hydrolysis (22). It can be purified on a large scale by a combination of silica, ion-exchange, and reverse-phase chromatography. As shown in Figs. 2–5, intact Kdo_2-Lipid A from *E. coli* WBB06 is amenable to full structural analysis by high-resolution ESI/MS and NMR methodology. It has demonstrated stability for 9 months as the ammonium salt, when stored neat in ampoules at −16°C to −24°C. Extended stability studies are ongoing. Over 99% of the purified material is hexa-acylated, with ~91% as compound A, ~5% as B, and 3% as F (Figs. 1–3).

Murphy et al. (21) have recently detected trace amounts of *E. coli* Kdo_2-Lipid A species that contain odd-chain fatty acids, which might arise by the priming of fatty acid biosynthesis with propionyl-CoA instead of acetyl-CoA (45). It is unlikely that these species or the other minor impurities detected (Figs. 2, 3) would have a significant impact on the biological activity of the major component, compound A (Fig. 1). In any event, these contaminants would also be present in all other *E. coli* or *Salmonella* LPS preparations.

The structural characterization of our Kdo_2-Lipid A exceeds that of any previously reported natural lipid A or LPS. Its biological activity is comparable to that of our current lot of Sigma L4130 LPS (from *E. coli* 0111:B4) made by conventional procedures (Figs. 6–10). The repro-

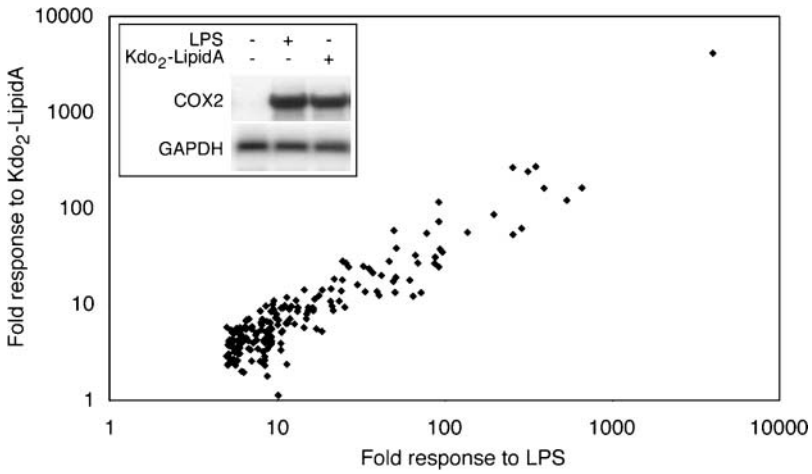

Fig. 10. Comparison of the effects of LPS and Kdo_2-Lipid A on gene expression in RAW 264.7 macrophages. RAW 264.7 cells were treated with 100 ng/ml LPS, 100 ng/ml Kdo_2-Lipid A, or the control buffer. Total RNA was collected 6 h following treatment and used for microarray analysis on Codelink Mouse Uniset 1 microarrays. The fold induction of the 200 most highly LPS-responsive genes is compared with the fold induction of these genes in response to Kdo_2-Lipid A. Inset: Northern blot analysis of total RNA (10 μg) isolated from control, LPS-treated or Kdo_2-Lipid A-treated RAW 264.7 cells for COX2 and GAPDH.

ducibility and chemically defined nature of our Kdo_2-Lipid A should make it very attractive as a standard for pharmaceutical quality control.

Although hexa-acylated *E. coli* lipid A by itself has significant biological activity, we chose to use Kdo_2-Lipid A (also termed ReLPS) for our studies, because it is supposedly ~10 times more potent than lipid A (8, 46), and it can be extracted directly from cells without the use of mild acid hydrolysis, which is required to remove the Kdo residues from lipid A (44, 47, 48). Treatment of LPS with mild acid introduces additional micro-heterogeneity into lipid A, such as the partial dephosphorylation of the 1 position or the elimination of an acyl chain (49). It is likely that Kdo_2-Lipid A is slightly more active than lipid A because it is dispersed more efficiently in aqueous systems. The availability of large amounts of Kdo_2-Lipid A should enable in-depth studies of lipid A physical properties in water, such as the determination of its critical micelle concentration, its phase behavior as a function of pH and various counter ions, and its formation of complexes with proteins. Such studies are underway (S. White, personal communication).

A significant advantage of Kdo_2-Lipid A over LPS is that it is a reproducible, well-defined substance that should be detectable with great sensitivity by ESI/MS and/or MRM after uptake by cultured macrophages or injection into animals. This feature will permit quantitative pharmacokinetic and metabolic studies, which are not possible with full-length LPS. In this context, it would be of interest to compare Kdo_2-Lipid A to LPS under the recently published human endotoxin infusion protocols (13, 15), given that plasma, urine, and circulating white cell levels of Kdo_2-Lipid A could be determined in parallel with markers of bioactivity. To facilitate quantification by mass spectrometry, it will be necessary to develop an additional external standard, such as a uniformly ^{13}C-labeled Kdo_2-Lipid A analog. Known amounts of this material would then be added to lipid mixtures extracted from plasma or tissues, and would allow for the quantification by mass spectrometry of any unlabeled Kdo_2-Lipid A present in such samples. A ^{13}C-labeled Kdo_2-Lipid A standard could easily be prepared form WBB06 cells grown on minimal medium with [U-^{13}C]glucose as their sole carbon source, using the purification protocols described above.

Kdo_2-Lipid A is an excellent substrate for diverse lipid A modification enzymes. For instance, Kdo_2-Lipid A is deacylated by PagL at the 3 position (50, 51), dephosphorylated by LpxE at the 1 position (52–54), modified by EptB with phosphoethanolamine on the outer Kdo unit (55), and modified with 4-amino-4-deoxy-L-arabinose by ArnT on the 4′ phosphate group (56). These enzymes can act singly or in combination. The many resulting derivatives of Kdo_2-Lipid A may prove useful as immuno-modulators, because some of these modifications are expected to alter the interactions of the lipid with TLR-4. For instance, the combined action of PagL and LpxE on Kdo_2-Lipid A generates the same lipid A substructure currently used in the clinic as an adjuvant (57, 58), but with the retention of the Kdo disaccharide. Our Kdo_2-Lipid A therefore provides an ideal starting material for exploring these and other chemo-enzymatic transformations.

A major remaining challenge in elucidating the function of innate immunity receptors is the determination of their three-dimensional structures in the presence of bound ligands. X-ray structures of TLR-3 and of CD14, both without bound ligands, have recently been reported (59, 60). In the case of TLR-4, a ternary complex with MD2 and Kdo_2-Lipid A would be especially informative (7). A solution structure of MD2 with Kdo_2-Lipid A might also be of considerable interest. We believe that our Kdo_2-Lipid A is of sufficient purity to merit consideration as a ligand for cocrystallization trials. The possibility of generating pure ^{13}C-labeled Kdo_2-Lipid A, as described above, should greatly facilitate NMR solution studies of complexes with MD2, or CD14. Heptose-deficient "Re" LPS from *Salmonella minnesota*, which is often used to stimulate immune cells, would not be suitable for such biophysical studies, because of its considerable micro-heterogeneity with regard to the number of acyl chains and polar substituents (48, 61, 62).

In summary, we have devised an efficient new purification scheme for obtaining large amounts Kdo_2-Lipid A from *E. coli* and have demonstrated its functionality in activating macrophage genes, eicosanoids, and cytokines. We believe that our analytical technology, especially the HPLC system shown in Fig. 2, will be applicable to diverse lipid A molecules of natural and synthetic origin. Entirely different saccharolipids, such as mycobacterial trehalose derivatives (63) or *Rhizbium* nodulation factors (64), could also be purified on a large scale and analyzed by our procedures.

This work was supported by the LIPID MAPS Large Scale Collaborative, Grant GM-069338 from the National Institutes of Health. We are grateful to the National Institutes of General Medical Sciences for supporting this effort.

REFERENCES

1. Dennis, E. A., H. A. Brown, R. Deems, C. K. Glass, A. H. Merrill, R. C. Murphy, C. R. H. Raetz, W. Shaw, S. Subramaniam, D. W. Russell, et al. 2005. The LIPID MAPS approach to lipidomics. *In.* Functional Lipidomics. L. Feng and G. D. Prestwich, editors. CRC Press/Taylor and Francis Group, Boca Raton, FL.1–15.
2. Murphy, R. C., J. Fiedler, and J. Hevko. 2001. Analysis of nonvolatile lipids by mass spectrometry. *Chem. Rev.* **101:** 479–526.
3. Pulfer, M., and R. C. Murphy. 2003. Electrospray mass spectrometry of phospholipids. *Mass Spectrom. Rev.* **22:** 332–364.
4. Fahy, E., S. Subramaniam, H. A. Brown, C. K. Glass, A. H. Merrill, Jr., R. C. Murphy, C. R. H. Raetz, D. W. Russell, Y. Seyama, W. Shaw, et al. 2005. A comprehensive classification system for lipids. *J. Lipid Res.* **46:** 839–862.
5. Aderem, A., and R. J. Ulevitch. 2000. Toll-like receptors in the induction of the innate immune response. *Nature.* **406:** 782–787.
6. Raetz, C. R. H., and C. Whitfield. 2002. Lipopolysaccharide endotoxins. *Annu. Rev. Biochem.* **71:** 635–700.
7. Gangloff, M., and N. J. Gay. 2004. MD-2: the Toll 'gatekeeper' in endotoxin signalling. *Trends Biochem. Sci.* **29:** 294–300.
8. Rietschel, E. T., T. Kirikae, F. U. Schade, U. Mamat, G. Schmidt, H. Loppnow, A. J. Ulmer, U. Zähringer, U. Seydel, F. Di Padova, et al. 1994. Bacterial endotoxin: molecular relationships of structure to activity and function. *FASEB J.* **8:** 217–225.

9. Brade, H., S. M. Opal, S. N. Vogel, and D. C. Morrison, editors. 1999. Endotoxin in Health and Disease. Marcel Dekker, Inc., New York.
10. Nikaido, H. 2003. Molecular basis of bacterial outer membrane permeability revisited. *Microbiol. Mol. Biol. Rev.* **67:** 593–656.
11. Ulevitch, R. J. 2004. Therapeutics targeting the innate immune system. *Nat. Rev. Immunol.* **4:** 512–520.
12. Visintin, A., K. A. Halmen, E. Latz, B. G. Monks, and D. T. Golenbock. 2005. Pharmacological inhibition of endotoxin responses is achieved by targeting the TLR4 coreceptor, MD-2. *J. Immunol.* **175:** 6465–6472.
13. Lynn, M., D. P. Rossignol, J. L. Wheeler, R. J. Kao, C. A. Perdomo, R. Noveck, R. Vargas, T. D'Angelo, S. Gotzkowsky, and F. G. McMahon. 2003. Blocking of responses to endotoxin by E5564 in healthy volunteers with experimental endotoxemia. *J. Infect. Dis.* **187:** 631–639.
14. Prabhakar, U., T. M. Conway, P. Murdock, J. L. Mooney, S. Clark, P. Hedge, B. C. Bond, E. C. Jazwinska, M. R. Barnes, F. Tobin, et al. 2005. Correlation of protein and gene expression profiles of inflammatory proteins after endotoxin challenge in human subjects. *DNA Cell Biol.* **24:** 410–431.
15. Calvano, S. E., W. Xiao, D. R. Richards, R. M. Felciano, H. V. Baker, R. J. Cho, R. O. Chen, B. H. Brownstein, J. P. Cobb, S. K. Tschoeke, et al. 2005. A network-based analysis of systemic inflammation in humans. *Nature.* **437:** 1032–1037.
16. Hawkins, L. D., W. J. Christ, and D. P. Rossignol. 2004. Inhibition of endotoxin response by synthetic TLR4 antagonists. *Curr. Top. Med. Chem.* **4:** 1147–1171.
17. Golenbock, D. T., R. Y. Hampton, N. Qureshi, K. Takayama, and C. R. H. Raetz. 1991. Lipid A-like molecules that antagonize the effects of endotoxins on human monocytes. *J. Biol. Chem.* **266:** 19490–19498.
18. Bryans, T. D., C. Braithwaite, J. Broad, J. F. Cooper, K. R. Darnell, V. M. Hitchins, A. J. Karren, and P. S. Lee. 2004. Bacterial endotoxin testing: a report on the methods, background, data, and regulatory history of extraction recovery efficiency. *Biomed. Instrum. Technol.* **38:** 73–78.
19. Cohen, J. 2000. The detection and interpretation of endotoxaemia. *Intensive Care Med.* **26 (Suppl. 1):** 51–56.
20. Brabetz, W., S. Muller-Loennies, O. Holst, and H. Brade. 1997. Deletion of the heptosyltransferase genes *rfaC* and *rfaF* in *Escherichia coli* K-12 results in an Re-type lipopolysaccharide with a high degree of 2-aminoethanol phosphate substitution. *Eur. J. Biochem.* **247:** 716–724.
21. Murphy, R. C., C. R. H. Raetz, C. M. Reynolds, and R. M. Barkley. 2005. Mass spectrometry advances in lipidomica: collision-induced decomposition of Kdo(2)-lipid A. *Prostaglandins Other Lipid Mediat.* **77:** 131–140.
22. Kanipes, M. I., S. Lin, R. J. Cotter, and C. R. H. Raetz. 2001. Ca2+-induced phosphoethanolamine transfer to the outer 3-deoxy-D-manno-octulosonic acid moiety of *Escherichia coli* lipopolysaccharide. A novel membrane enzyme dependent upon phosphatidylethanolamine. *J. Biol. Chem.* **276:** 1156–1163.
23. Folch, J., M. Lees, and G. H. Sloane Stanley. 1957. A simple method for the isolation and purification of total lipides from animal tissues. *J. Biol. Chem.* **226:** 497–509.
24. Ribeiro, A. A., Z. Zhou, and C. R. H. Raetz. 1999. Multi-dimensional NMR structural analyses of purified lipid X and lipid A (endotoxin). *Magn. Reson. Chem.* **37:** 620–630.
25. Que, N. L. S., A. A. Ribeiro, and C. R. H. Raetz. 2000. Two-dimensional NMR spectroscopy and structures of six lipid A species from *Rhizobium etli* CE3. Detection of an acyloxyacyl residue in each component and origin of the aminogluconate moiety. *J. Biol. Chem.* **275:** 28017–28027.
26. Zhou, Z., A. A. Ribeiro, and C. R. H. Raetz. 2000. High-resolution NMR spectroscopy of lipid A molecules containing 4-amino-4-deoxy-L-arabinose and phosphoethanolamine substituents. Different attachment sites on lipid A molecules from NH_4VO_3-treated *Escherichia coli* versus kdsA mutants of *Salmonella typhimurium*. *J. Biol. Chem.* **275:** 13542–13551.
27. Hoshino, K., O. Takeuchi, T. Kawai, H. Sanjo, T. Ogawa, Y. Takeda, K. Takeda, and S. Akira. 1999. Cutting edge: Toll-like receptor 4 (TLR4)-deficient mice are hyporesponsive to lipopolysaccharide: evidence for TLR4 as the Lps gene product. *J. Immunol.* **162:** 3749–3752.
28. Akira, S., and K. Takeda. 2004. Toll-like receptor signalling. *Nat. Rev. Immunol.* **4:** 499–511.
29. Valledor, A. F., L. C. Hsu, S. Ogawa, D. Sawka-Verhelle, M. Karin, and C. K. Glass. 2004. Activation of liver X receptors and retinoid X receptors prevents bacterial-induced macrophage apoptosis. *Proc. Natl. Acad. Sci. USA.* **101:** 17813–17818.
30. Ogawa, S., J. Lozach, C. Benner, G. Pascual, R. K. Tangirala, S. Westin, A. Hoffmann, S. Subramaniam, M. David, M. G. Rosenfeld, et al. 2005. Molecular determinants of crosstalk between nuclear receptors and toll-like receptors. *Cell.* **122:** 707–721.
31. Brozek, K. A., K. Hosaka, A. D. Robertson, and C. R. H. Raetz. 1989. Biosynthesis of lipopolysaccharide in *Escherichia coli*: cytoplasmic enzymes that attach 3-deoxy-D-*manno*-octulosonic acid to lipid A. *J. Biol. Chem.* **264:** 6956–6966.
32. Grandori, C., S. M. Cowley, L. P. James, and R. N. Eisenman. 2000. The Myc/Max/Mad network and the transcriptional control of cell behavior. *Annu. Rev. Cell Dev. Biol.* **16:** 653–699.
33. Poltorak, A., X. He, I. Smirnova, M. Y. Liu, C. V. Huffel, X. Du, D. Birdwell, E. Alejos, M. Silva, C. Galanos, et al. 1998. Defective LPS signaling in C3H/HeJ and C57BL/10ScCr mice: mutations in Tlr4 gene. *Science.* **282:** 2085–2088.
34. Galanos, C., O. Lüderitz, and O. Westphal. 1969. A new method for the extraction of R lipopolysaccharides. *Eur. J. Biochem.* **9:** 245–249.
35. Westphal, O., and K. Jann. 1965. Bacterial lipopolysaccharides: extraction with phenol-water and further application of the procedure. In *Methods in Carbohydrate Chemistry 5:* R. L. Whistler, editor. Academic Press. New York, NY. 83–91.
36. Goldman, R. C., and L. Leive. 1980. Heterogeneity of antigenic side-chain length in lipopolysaccharide from *Escherichia coli* O111 and *Salmonella typhimurium* LT2. *Eur. J. Biochem.* **107:** 145–153.
37. Lebbar, S., D. Karibian, C. Deprun, and M. Caroff. 1994. Distribution of lipid A species between long and short chain lipopolysaccharides isolated from *Salmonella*, *Yersinia*, and *Escherichia* as seen by ^{252}Cf plasma desorption mass spectrometry. *J. Biol. Chem.* **269:** 31881–31884.
38. Imoto, M., H. Yoshimura, N. Sakaguchi, T. Shimamoto, S. Kusumoto, and T. Shiba. 1987. Total synthesis of *Escherichia coli* lipid A, the endotoxically active principle of cell-surface lipopolysaccharide. *Bull. Chem. Soc. Jpn.* **60:** 2205–2214.
39. Yoshizaki, H., N. Fukuda, K. Sato, M. Oikawa, K. Fukase, Y. Suda, and S. Kusumoto. 2001. First total synthesis of the Re-type lipopolysaccharide. *Angew. Chem. Int. Ed. Engl.* **40:** 1475–1480.
40. Christ, W. J., P. D. McGuinness, O. Asano, Y. Wang, M. A. Mullarkey, M. Perez, L. D. Hawkins, T. A. Blythe, G. R. Dubuc, and A. L. Robidoux. 1994. Total synthesis of the proposed structure of *Rhodobacter sphaeroides* lipid A resulting in the synthesis of a new potent lipopolysaccharide antagonist. *J. Am. Chem. Soc.* **116:** 3637–3638.
41. Christ, W. J., O. Asano, A. L. Robidoux, M. Perez, Y. Wang, G. R. Dubuc, W. E. Gavin, L. D. Hawkins, P. D. McGuinness, M. A. Mullarkey, et al. 1995. E5531, a pure endotoxin antagonist of extraordinary potency: chemistry and biology. *Science.* **265:** 80–83.
42. Plante, O. J., and P. H. Seeberger. 2003. Recent advances in automated solid-phase carbohydrate synthesis: from screening to vaccines. *Curr. Opin. Drug Discov. Devel.* **6:** 521–525.
43. Seeberger, P. H., and D. B. Werz. 2005. Automated synthesis of oligosaccharides as a basis for drug discovery. *Nat. Rev. Drug Discov.* **4:** 751–763.
44. Rosner, M. R., J. Tang, I. Barzilay, and H. G. Khorana. 1979. The structure of lipopolysaccharide from an *Escherichia coli* heptose-less mutant. III. Two fatty acyl amidases from *Dictyostelium discoideum* and their action on lipopolysaccharide derivatives. *J. Biol. Chem.* **254:** 5906–5917.
45. Magnuson, K., S. Jackowski, C. O. Rock, and J. E. Cronan, Jr. 1993. Regulation of fatty acid biosynthesis in *Escherichia coli.Microbiol. Rev.* **57:** 522–542.
46. Loppnow, H., H. Brade, I. Dürrbaum, C. A. Dinarello, S. Kusumoto, E. T. Rietschel, and H. D. Flad. 1989. IL-1 induction capacity of defined lipopolysaccharide partial structures. *J. Immunol.* **142:** 3229–3238.
47. Zhou, Z., S. Lin, R. J. Cotter, and C. R. H. Raetz. 1999. Lipid A modifications characteristic of *Salmonella typhimurium* are induced by NH_4VO_3 in *Escherichia coli* K12. Detection of 4-amino-4-deoxy-L-arabinose, phosphoethanolamine and palmitate. *J. Biol. Chem.* **274:** 18503–18514.
48. Zhou, Z., A. A. Ribeiro, S. Lin, R. J. Cotter, S. I. Miller, and C. R. H. Raetz. 2001. Lipid A modifications in polymyxin-resistant *Salmonella typhimurium*: PMRA-dependent 4-amino-4-deoxy-L-arabinose and phosphoethanolamine incorporation. *J. Biol. Chem.* **276:** 43111–43121.

49. Qureshi, N., K. Takayama, and E. Ribi. 1982. Purification and structural determination of non-toxic lipid A obtained from the lipopolysaccharide of *Salmonella typhimurium*. *J. Biol. Chem.* **257:** 11808–11815.
50. Trent, M. S., W. Pabich, C. R. H. Raetz, and S. I. Miller. 2001. A PhoP/PhoQ-induced lipase (PagL) that catalyzes 3-*O*-deacylation of lipid A precursors in membranes of *Salmonella typhimurium*. *J. Biol. Chem.* **276:** 9083–9092.
51. Raetz, C. R. H. 2001. Regulated covalent modifications of lipid A. *J. Endotoxin Res.* **7:** 73–78.
52. Karbarz, M. J., S. R. Kalb, R. J. Cotter, and C. R. H. Raetz. 2003. Expression cloning and biochemical characterization of a *Rhizobium leguminosarum* lipid A 1-phosphatase. *J. Biol. Chem.* **278:** 39269– 39279.
53. Tran, A. X., M. J. Karbarz, X. Wang, C. R. H. Raetz, S. C. McGrath, R. J. Cotter, and M. S. Trent. 2004. Periplasmic cleavage and modification of the 1-phosphate group of Helicobacter pylori lipid A. *J. Biol. Chem.* **279:** 55780–55791.
54. Wang, X., M. J. Karbarz, S. C. McGrath, R. J. Cotter, and C. R. H. Raetz. 2004. MsbA transporter-dependent lipid A 1-dephosphorylation on the periplasmic surface of the inner membrane: topography of francisella novicida LpxE expressed in *Escherichia coli*. *J. Biol. Chem.* **279:** 49470–49478.
55. Reynolds, C. M., S. R. Kalb, R. J. Cotter, and C. R. H. Raetz. 2005. A phosphoethanolamine transferase specific for the outer 3-deoxy-D-*manno*-octulosonic acid residue of *Escherichia coli* lipopolysaccharide. Identification of the *eptB* gene and Ca2+ hypersensitivity of an *eptB* deletion mutant. *J. Biol. Chem.* **280:** 21202–21211.
56. Trent, M. S., A. A. Ribeiro, S. Lin, R. J. Cotter, and C. R. H. Raetz. 2001. An inner membrane enzyme in *Salmonella typhimurium* and *Escherichia coli* that transfers 4-amino-4-deoxy-L-arabinose to lipid A: induction in polymyxin-resistant mutants and role of a novel lipid-linked donor. *J. Biol. Chem.* **276:** 43122–43131.
57. Persing, D. H., R. N. Coler, M. J. Lacy, D. A. Johnson, J. R. Baldridge, R. M. Hershberg, and S. G. Reed. 2002. Taking toll: lipid A mimetics as adjuvants and immunomodulators. *Trends Microbiol.* **10 (Suppl.):** 32–37.
58. Baldridge, J. R., P. McGowan, J. T. Evans, C. Cluff, S. Mossman, D. Johnson, and D. Persing. 2004. Taking a Toll on human disease: Toll-like receptor 4 agonists as vaccine adjuvants and monotherapeutic agents. *Expert Opin. Biol. Ther.* **4:** 1129–1138.
59. Choe, J., M. S. Kelker, and I. A. Wilson. 2005. Crystal structure of human toll-like receptor 3 (TLR3) ectodomain. *Science.* **309:** 581–585.
60. Kim, J. I., C. J. Lee, M. S. Jin, C. H. Lee, S. G. Paik, H. Lee, and J. O. Lee. 2005. Crystal structure of CD14 and its implications for lipopolysaccharide signaling. *J. Biol. Chem.* **280:** 11347–11351.
61. Qureshi, N., P. Mascagni, E. Ribi, and K. Takayama. 1985. Monophosphoryl lipid A obtained from lipopolysaccharides of Salmonella minnesota R595. Purification of the dimethyl derivative by high performance liquid chromatography and complete structural determination. *J. Biol. Chem.* **260:** 5271–5278.
62. Boll, M., J. Radziejewska-Lebrecht, C. Warth, D. Krajewska-Pietrasik, and H. Mayer. 1994. 4-Amino-4-deoxy-L-arabinose in LPS of enterobacterial R-mutants and its possible role for their polymyxin reactivity. *FEMS Immunol. Med. Microbiol.* **8:** 329–341.
63. Brennan, P. J., and H. Nikaido. 1995. The envelope of mycobacteria. *Annu. Rev. Biochem.* **64:** 29–63.
64. Denarie, J., F. Debelle, and J-C. Prome. 1996. *Rhizobium* lipochitooligosaccharide nodulation factors: signalling molecules mediating recognition and morphogenesis. *Annu. Rev. Biochem.* **65:** 503–535.
65. Clementz, T., Z. Zhou, and C. R. H. Raetz. 1997. Function of the *Escherichia coli msbB* gene, a multicopy suppressor of *htrB* Knockouts, in the acylation of lipid A. Acylation by MsbB follows laurate incorporation by HtrB. *J. Biol. Chem.* **272:** 10353–10360.
66. Vorachek-Warren, M. K., S. Ramirez, R. J. Cotter, and C. R. H. Raetz. 2002. A triple mutant of *Escherichia coli* lacking secondary acyl chains on lipid A. *J. Biol. Chem.* **277:** 14194–14205.
67. Bishop, R. E., H. S. Gibbons, T. Guina, M. S. Trent, S. I. Miller, and C. R. H. Raetz. 2000. Transfer of palmitate from phospholipids to lipid A in outer membranes of Gram-negative bacteria. *EMBO J.* **19:** 5071–5080.